JANUARY 31 2005

A study of active tonal noise control for a small axial flow fan

J. Wang; L. Huang; L. Cheng

J. Acoust. Soc. Am. 117, 734–743 (2005)
https://doi.org/10.1121/1.1848072

A study of active tonal noise control for a small axial flow fan

J. Wang, L. Huang,[a] and L. Cheng
Department of Mechanical Engineering, The Hong Kong Polytechnic University, Kowloon, Hong Kong

(Received 2 July 2004; revised 9 November 2004; accepted 11 November 2004)

Sound radiated by a computer cooling fan consists of tones which are phase locked with the rotation, and other less deterministic tones and broadband random noise. This paper demonstrates the feasibility of globally eliminating the rotation-locked tones by applying a very simple destructive interference to a modified cooling fan with the number of struts equal to the number of rotor blades. The rig consists of a miniature electret microphone used as a rotation sensor, an ordinary loudspeaker, and a bandpass filter with adjustable amplitude and phase delay. The microphone is located at the inlet bellmouth of the fan to pick up the fluctuating aerodynamic pressure caused by the passing rotor blades. The pressure spectrum is rich in the blade passing frequency (BPF) and its low-order harmonics. It provides much better performance than a pulse-generating tachometer. Analysis of the original fan noise shows that about 90% of the radiated tonal sound is phase locked with rotation, and this portion is almost completely eliminated in all directions. The reductions of the radiated sound power in the first two BPFs are 18.5 and 13.0 dB, respectively, and the overall sound power reduction is 11.0 dB. © *2005 Acoustical Society of America.*
[DOI: 10.1121/1.1848072]

PACS numbers: 43.50.Ki, 43.28.Ra, 43.50.Ed [SFW] Pages: 734–743

I. INTRODUCTION

Knowledge of generic fan noise mechanisms exists but it may be said that the abatement of noise from a specific fan application remains a tough job. This study is concerned with the feasibility of applying the technique of destructive acoustic interference to a computer cooling fan, and the primary motivation for the study is to maximize the simplicity and the global effectiveness of the technique so that it might become economic enough to be applied in practice. In this section, the general fan noise mechanisms are given a brief review, together with efforts to reduce the fan noise. This is then followed by the rationale for the choice of the specific fan configuration and the active control technique.

A. General fan noise mechanisms

Fans are but one member of the turbomachinery family and, as far as the acoustics is concerned, the family may also include helicopter rotors and propellers. The study of the propeller noise caused by the steady loading was the topic of Gutin's (1936) research. In the application of fan noise, Gutin noise is negligible. The dominant noise source is the dipole caused by the fluctuating pressure on the rotating blades. The study of Tyler and Sofrin (1962) was significant in that it revealed the paramount importance of the matching or mismatching of the numbers of the rotor and stator blades for the noise caused by the rotor–stator interaction. A rather formal theoretical platform was established by Lighthill's (1952) acoustic analogy for the aerodynamic noise caused by a compact turbulent jet, and its elegant extension by Ffowcs Williams and Hawkings (1969) to applications where the presence of a solid structure in arbitrary motion is a primary feature. Since then the use of the so-called Ffowcs Williams and Hawkings equation has served well the community of turbomachinery noise research although alternative approaches also exist. In fact, search for the knowledge of a specific fan noise mechanism has never ceased since Gutins time, and reviews of the topic at large were written by authors such as Sharland (1964) and Morfey (1973). The work of Lowson (1965, 1970) on the point source formulation for the unducted rotors was, in the opinion of the current authors, quite useful and illuminating. These formulations were recently adapted to characterize the specific application of computer cooling fans (Huang, 2003) where the numbers of rotor and stator blades are small. Focusing on computer cooling fans, the important mechanisms of fan noise are summarized below.

- Tip leakage flow. The flow leaks through the blade tip due to the pressure difference developed between the pressure and suction sides of a blade. The leakage flow may manifest itself into jetlike, unstable shear layers and roll up into vortices in the blade passage. It may even hit a neighboring blade. Details can be found in the work of Fukano *et al.* (1986), among others.
- Nonuniform inlet flow condition. A nonuniform inlet flow is seen as unsteady flow by rotating blades and unsteady pressure ensues on the blade surfaces. This is perhaps one of the most efficient dipole sources of fan noise. The noise thus radiated is often a combination of broadband and tones (Trunzo *et al.*, 1981; Majumdar and Peake, 1998).
- Turbulent and/or separated flow condition on a rotor. Flow separation occurs whenever the incidence angle is large, and most realistic flows through a fan are more or less always turbulent. Large scale flow turbulence, such as that caused by a fan working at a loading much higher than the condition it is designed for, can be very noisy, and most of the noise created is broadband in nature [see, for example, Sharland (1964) and Longhouse (1976)].

[a]Author to whom correspondence should be addressed. Electronic mail: mmlhuang@polyu.edu.hk

- Trailing edge noise. When unstable convection waves inside a developing boundary layer are disrupted by the trailing edge of a blade, part of the energy is scattered into sound waves (Ffowcs Williams and Hall, 1970). The resulting sound power is proportional to the fifth power of the representative flow speed when the source is noncompact, and the dependency becomes the sixth power when the source is compact (Howe, 1998; Blake, 1986).
- Rotor-stator interaction. When the wake of a rotor impinges on the stator blades, forces on the stator blades fluctuate rapidly. Empirical models for such interaction (Kemp and Sears, 1953, 1955) have still served the purpose of noise estimation. This is often the dominant noise source in turbomachinery. Recently, Huang (2003) speculated that the back reaction towards the upstream blade row could be more important when the downstream stator is a bluff body like a circular strut used in computer cooling fans. The unsteady force generated on the upstream rotor is caused by the periodic flow blockage by the downstream struts.

B. Fan noise abatement

Sound absorption is often the most reliable and effective measure of noise abatement, but this is not true for unducted fan applications. Most efforts of fan noise abatement have been directed towards improving the flow conditions pertinent to noise source mechanisms, such as the inlet flow uniformity, and the reduction of the strength of wake interactions which depend crucially on the distance between the rotor and stator blades. Fitzgerald and Lauchle (1984) demonstrated a collection of modifications for reducing the axial flow fan noise, such as the use of a bellmouth to smooth out the inlet flow distortions, the leaning design of the downstream struts to reduce rotor-stator flow interactions, and the correction of the cupped trailing edge to prevent flow separation and vortex shedding. The method of leaning strut design was also discussed by Envia and Nallasamy (1999). They also showed that a positive sweep angle can reduce the tone level due to the additional cancellation caused by phase differences in the axial direction. Longhouse (1978) also attempted to eliminate the tip leakage flow by using a rotating shroud, a feature which may cause structural vibration problems if the shroud is not properly balanced.

In the area of active noise control (ANC), the technique has been tried for ducted fan with some success. The cut-on of the spinning pressure modes is first described by Tyler and Sofrin (1962) and the acoustics is essentially identical to that of duct acoustics. To cancel the sound of higher order modes propagating in a duct, Gerhold (1997) used a delicate ring of 48 microphones and many control sources in a duct. Thomas *et al.* (1993, 1994) controlled the plane wave mode in a duct by 12 electromagnetic compression sound drivers, and used three-channel feedforward method to create a 30° quiet zone for an operational turbofan engine. For unducted fan noise, ANC has not been tested as extensively. The main reason could be as follows. Noise from an unducted fan has complex modal composition in space, and it is rather hard to match such distribution with a limited number of secondary sources. Lauchle *et al.* (1997) and Quinlan (1992) have both had some success in suppressing the BPF tones of a fan in isolation except that a baffle was used on the rotational plane and that might have significantly changed the acoustic directivity of the fan. The work of Lauchle *et al.* (1997) is also remarkable in that the fan itself was shaken in the axial direction to serve as a control source. Apparently it was hoped that the vibrating fan would produce a good directivity match with the original noise pattern. The acoustic radiation from an oscillating fan can be thought of as follows. First, a vibrating fan assembly radiates noise much like a loudspeaker in the absence of flow. Second, the fact that the fan also shakes the flow means that it would induce additional fluid loading hence dipole radiation from the fan. Details of such flow modification by the fan oscillation are apparently beyond the scope of Lauchle *et al.* (1997). Generally speaking, it can be said that the modification could reduce or eliminate the unsteady loading on the fan structure caused by the wake interactions. It may also generate an antisound which matches with the original noise without directly interfering with the source of the original noise. Nauhaus *et al.* (2003) placed small flow obstructions around the blade tips, and blew air jets into the tip clearance. An active aerodynamic control algorithm was used to counter the rotating instability and suppress the BPF noise originating from the wake interactions. Similar aerodynamic control was also demonstrated by Rao *et al.* (2001) and Simonich *et al.* (1993). The work reported here shares the acoustic feature of the active noise control described above, but the use of formal control algorithms is deemphasized in favor of simplicity and the use of knowledge of specific source mechanisms.

C. Rationale for the current work

Instead of following the strategy of complex aerodynamic control, or using complex secondary loudspeaker arrays, this study aims to explore the feasibility of a very simple destructive acoustic interference technique for typical computer cooling fans which consist of a rotor and a set of downstream struts. The technique involves a redesign of the fan struts so that the primary noise becomes a simple dipole in the axial direction. A miniature microphone is used to pick up the information of blade rotation, much like a traditional tachometer, and the signal is filtered, phase shifted, and amplified to drive a single loudspeaker placed just beneath the fan casing. There is no error microphone and the setup can be regarded as a simple feedforward, open-loop control. The secondary noise is a simple dipole with its axis aligned with that of the fan rotation. The key questions asked are as follows. (a) How effective is the manipulation of the fan noise directivity? (b) Can the simplified noise be cancelled by the simple open-loop arrangement? The rationale for using such a simple scheme is based on practical considerations. One cannot afford to have a sophisticated control algorithm and complex detection and error microphones for applications like computer cooling. The same applies to many other situations.

In what follows in Sec. II, the noise made by the sample fan is analyzed thoroughly. The analysis shows the directivity, the components of noise that can be controlled, and those lying beyond the scope of the current scheme. It would also

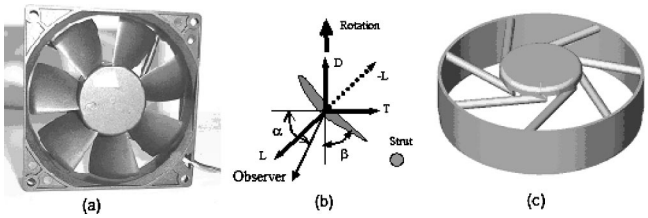

FIG. 1. Computer cooling fan and its noise sources. (a) is the front view of a typical fan, (b) is the cross-sectional view of a blade with forces acting on the surrounding air ($-L$) decomposed into thrust (T) and drag (D) components, and (c) is the strut design for the coincident configuration of $B=S=7$.

assess whether such a specially designed configuration with a dipole sound radiation is worthwhile for practical use. In Sec. III, details of the experimental configuration will be disseminated before the results of noise reduction are given. Such details include the sensor signal, loudspeaker performance, and the characteristics of the filters. At the end, results of the noise reduction and the limitations of the method are presented.

II. ANALYSIS OF THE ORIGINAL NOISE

A. Noise mechanisms of the sample cooling fan

As shown in Fig. 1(a), the sample fan for the study is a computer cooling fan of 92 mm in diameter, consisting of seven blades and four struts at the back for holding the motor. At the design point, the rotational speed is 3200 rpm. With such low blade tip speed, noise generated by the Gutin mechanisms is totally negligible. The acoustic spectrum consists of a broadband noise and discrete tones at the multiples of the blade passing frequency (BPF). As described by Wong and Huang (2003), the dominant noise source for such a fan is the aerodynamic interactions induced by two noticeable features. One is the interaction between the rotor blades and the downstream struts; another is the interaction between the distorted inlet flow pattern and the rotor, the inlet flow being a four-lobe distortion caused by the four sharp edges of the incomplete bellmouth cut short by the square outer frame. The dominant noise source is the fluctuating force induced by the two interaction processes on the rotor blades. If one compares the noises made by these two interactions, it is possible that the inlet flow distortion is louder. However, this feature can be avoided by using a complete and smooth bellmouth. As a result, the current study focuses on the noise radiated by the interaction between the rotor and its downstream struts, the latter being regarded as an essential structural feature that cannot be removed or drastically modified.

It has to be said that noise emanates from both blade surfaces and all other stationary surfaces experiencing unsteady pressure. However, the lift-generating nature of the rotor blade makes it the largest source of noise. Figure 1(b) is the cross-sectional view of a blade, and the unsteady force exerted on the surrounding air, which is the reaction of the lift, $-L$, is divided into two components: drag D and thrust T. The component of drag should be better named the driving force in this case but the term is kept here in step with literature. If the blade has a significant lean, a radial force component may also exist (not shown). The reason why the force is divided this way is that noise radiated by each of these components has its own distinct characters which can be used for the source characterization purpose. If the unsteady force on the blades is represented by a point force of thrust component T and drag component D, the rotary noise at the frequency of the mth harmonic of the fundamental BPF is given below in terms of its complex pressure amplitude c_{mB} (Lowson, 1965, 1970):

$$c_{mB}=\frac{imB\omega}{2\pi c_0 r_0}\sum_{k=-\infty}^{\infty} i^{-\nu}\left(T_{kS}\cos\alpha-\frac{\nu}{mBM}D_{kS}\right)\times J_\nu(mBM\sin\alpha),\quad \nu=mB-kS, \tag{1}$$

where B and S denote the numbers of the rotor blades and struts, respectively, ω is the angular rotating speed, mB is the frequency index of the observed sound, kS is the frequency index in the spectrum of the unsteady force, the dimensional frequency being the product of these indices and the rotational frequency, rps=rpm/60, r_0 is the distance between the fan center and the observer, α is the angle between the rotational axis and the observer direction, as shown in Fig. 1(b), c_0 is the speed of sound, M is the Mach number of the source point motion, and T_{kS}, D_{kS} are, respectively, the kS components of the spectra of the source forces T and D. Note that both m and k can be any integer. The frequency index differential, $\nu=mB-kS$, or the index of spinning pressure mode (Tyler and Sofrin, 1962) is the most important parameter. The source frequency index is kS because each blade experiences blockage by S struts during one cycle of rotation. The observed noise has frequency indices of mB because the noise of other frequency components is cancelled among themselves since B rotor blades all radiate sound with a fixed phase relation determined by the rotation. In fact, the phase relation is an important assumption which is not satisfied completely in reality. For example, there might be unsteady forces arising from vortex shedding from the cylinder and its timing could be very different from the fan rotation. Noise from such dynamic process cannot be modeled easily but can be measured and analyzed to some extent. Here, the part of noise that is phase locked to or synchronized with the rotation is denoted rotary noise, while the rest is denoted as random noise although the underlying mechanism could well be deterministic. The acoustic interference designed in this study deals solely with the rotary noise.

When the two indices coincide, $mB=kS$, the noise is rather loud since noises radiated by all blade-strut interaction events simply add up. This radiation is denoted here as the coincident mode, and the special design of $B=S$ allows such coincident radiation for all harmonics, $m=1,2,3,\ldots$. The coincident configuration is the one being tested in this study. The reason why noise is also made when the two frequency indices do not match, $\nu=mB-kS\neq 0$, is due to the Doppler effect of the source motion with the rotating blade. The strength of the Doppler effect is governed by the Bessel function $J_\nu(z)$ of order ν and argument $z=mBM\sin\alpha$. For the small cooling fan operating at low speed, normally BM

<0.2, the Bessel function can be simplified: $J_0|_{z\to 0}\to 1$, $J_{\pm 1}|_{z\to 0}\to 0.54z$.

It is clear that the thrust noise is loudest when $\nu=0$. However, examination of the drag noise term in Eq. (1) reveals a different phenomenon. The noise at $\nu=0$ is annulled by the presence of ν in the numerator, but the noise with $\nu=\pm 1$ is not proportional to z due to the presence of $mBM\propto z$ in the denominator. In fact, the loudest drag noise is heard when $\nu=\pm 1$ and the amplitude of the drag noise is of the same order (z^0) as that of the thrust noise in terms of the small argument z. This mode of drag noise radiation can be called the leading-order radiation, which is, in principle, equally noisy as the coincident mode thrust noise. This shift in coincident radiation mode originates from the artificial decomposition of the total fluctuating lift into D and T. The drag force D changes direction once per cycle and this changes the actual frequency perceived on the ground from kS to $kS\pm 1$, hence the loud noise at $\nu=\pm 1$. The reason why drag noise vanishes at $\nu=0$ is also rooted in its changing force direction, and detailed explanation is given by Huang (2003). Ideally, a quiet fan should be designed in such a way that the index $|\nu|$ is at least 2 or above for all integer numbers k. But a simple analysis of $\nu=mB-kS$ shows that this is almost impossible for the leading BPF harmonics, say $m=1, 2, 3$, when B and S are both small as might be limited by aerodynamic and structural considerations.

B. Acoustics of the coincident configuration

The knowledge of loud noise radiation with $\nu=0$ seems to be well known for most engineering designers of cooling fans, but that loud noise is also made with a design of $\nu=\pm 1$ does not seem to be as commonly known. This perhaps explains why the most popular design is $B=7$ with $S=4$, as shown in Fig. 1(a). The dominant BPF noise ($m=1$) occurs for $k=2$, $\nu=-1$, which is a loud drag noise. The drag noise radiated by such a mode has its peaks on the rotational plane, as indicated by the directivity factor of $\sin(\alpha)$ in Eq. (1), where α is the angle between the rotational axis and the source-observer vector. The drag source is in fact a rotating dipole which changes the axis constantly on the rotational plane. In contrast, a thrust noise is a dipole with a fixed axis which coincides with the rotational axis, for which the sound pressure directivity is $\cos(\alpha)$. If conventional loudspeakers are used to construct antisound, a ring of loudspeakers with delicate phase relation may be required to cancel the drag noise, while one fixed loudspeaker is all it takes for the thrust noise. This is the reason why a coincident design of $B=S$ is chosen for the current study. Figure 1(c) shows the design of struts. Note that, for such a configuration, all drag noise is cancelled out by the rotating blades and does not need any attention.

It has to be acknowledged that the increased number of struts increases the time-mean blockage of the flow, and the aerodynamic performance of the fan may suffer. In fact, the actual amount of noise radiated by this coincident design of $B=S=7$ would also be higher than the leading order drag noise radiation of the original design, $B=7$, $S=4$. A specific estimate of the sound powers from the two configurations was made in (Wong and Huang, 2003) and a general analysis

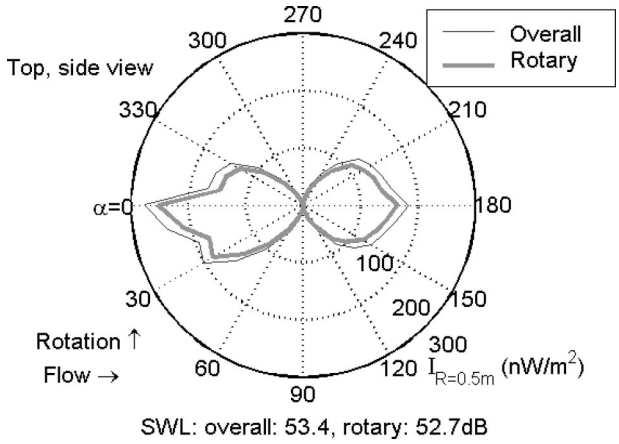

FIG. 2. Directivity of the sound intensity measured at $r_0=0.5$ m when the sample fan operates at 3200 rpm.

is given for the effect of S by Huang (2003), both concluding that S is a very dominant factor when the size of each strut is fixed. However, the conclusion changes if the size of each strut is allowed to decrease. For $S=7$, the strut size could be cut down to $\frac{4}{7}$ of the original. In such a case, one strut may not be able to contain all the electrical wires, and two struts might be involved for wiring. This issue of practical design complication is put aside for the moment. Wong and Huang (2003) also found that the lift fluctuation T_{kS} is almost proportional to d^x where d is the strut diameter and $x>2$. So the reduction in strut size by a factor of $\frac{4}{7}$ would give a noise reduction of at least $20\log_{10}(\frac{7}{4})^2=9.7$ dB. This would, to a large extent, compensate for the difference between the coincident thrust noise and the leading-order drag noise radiation from $S=4$. In addition to this justification, there are cooling fans which feature fewer rotor blades, such as $B=3$ or 4. In such applications, the coincident design of $S=B$ may well be the best choice for structural reasons. In short, the design of $B=S$ is not unrealistic for a fan with few rotor blades, and the original strut size is used for demonstration purpose.

The directivity measured in the full anechoic chamber for the coincident configuration is shown in Fig. 2 in the form of sound intensity distribution when the fan operates at 3200 rpm. The intensity is calculated by the far field approximation, $I=p_{rms}^2/(\rho_0 c_0)$, where p_{rms} is the local rms value of the measured sound which contains the near field contribution. The exact intensity is $I=1/2\,\mathrm{Re}(pu_r^*)$, where u_r^* is the conjugate of the radial component of the acoustic particle velocity. For the sound field produced by a simple dipole, formulas for p and u_r can be found in Dowling (1998) for simulation purpose. When the sound power integration is carried out over a sphere of radius $r=0.5$ m from the fan center, the error caused by the sound intensity approximation is 9%, which means $10\log(1.09)=0.37$ dB. Due to the low sound pressure level in some part of the fan noise pattern, use of a large radius r would give a very poor microphone signal. Therefore $r=0.5$ m is used in measurement as a compromise. Comparing with sound pressure level, the use of intensity I in the directivity plot amplifies any nonuniformity existing in the actual acoustic field. The thin outer curve in

Fig. 2 is the intensity of the overall noise, the thicker inner line is the rotary component found by synchronous averaging with the help of a tachometer [see Wong and Huang (2003) for details]. The sound power level (SWL) is the result of integration of the sound intensity I, and details are given in Eq. (15) of Huang (2003). The total sound power levels (SWL ref. 10^{-12} W) for the two intensity distributions are indicated in the lower label. Note that the rotary noise dominates in this case. Note also that, when the inlet flow condition is smoothed out, the original fan with four struts shown in Fig. 1(a) has a sound power of around 47 dB, while the current coincident configuration has 53.4 dB, which is not too noisy considering the use of $S=7$ struts with its original size.

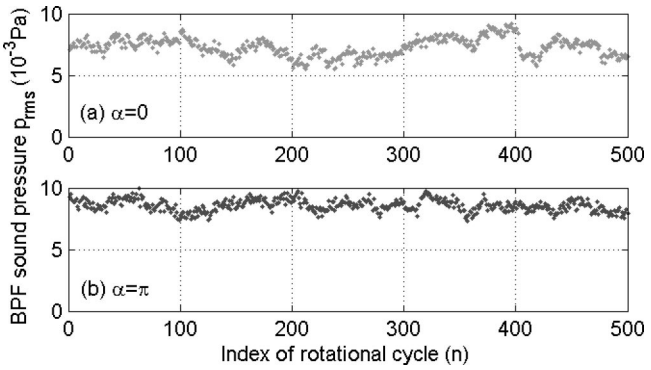

FIG. 3. The cycle-to-cycle variation of the BPF sound pressure amplitude in (a) the front and (b) the back of the fan.

C. Analysis of the noise components

Ideally, the sound radiated by the fan is a perfect thrust dipole with an intensity directivity of $I(\alpha)\propto\cos^2\alpha$, and the radiation is perfectly stable with a constant rpm. A single loudspeaker is then able to radiate a perfect antisound to cancel the fan noise. The reality deviates from this in many ways, and the part of noise that does conform to the ideal assumption is here called controllable noise. Major deviations are analyzed below.

First, the actual sound radiation does not feature T and D with equal strength on every blade with a perfect time difference locked with the rotation. Unsteady forces can hardly be deterministic given the high Reynolds number flow which is inevitably turbulent. If the force on one blade is different from the average of the seven blades, the difference can be seen as the effect of having an additional single strut, $S=1$, for which the noise of all sorts of spinning pressure mode ν exists including the drag noise. Second, the rotational speed varies from one cycle to the next slightly. Since the active control technique can only use the information from one cycle to construct antisound to cancel the noise of the next cycle, the imperfection of noise radiation caused by rotational speed variation is another source of uncontrollable noise. Since the directivity shown in Fig. 2 is taken by using a single microphone traversing the whole horizontal plane of 360°, its deviation from a perfect $\cos^2(\alpha)$ distribution is also partly attributed to the temporal variation of rotational speed and rotor-strut interaction. The extent to which the measured directivity $I(\alpha)$ conforms to the ideal distribution of, say, $I_T\cos^2\alpha$, may be measured by the following correlation calculation,

$$I_T=\int_0^{\pi} I(\alpha)\cos^2\alpha\, d\alpha \Big/ \int_0^{\pi}\cos^4\alpha\, d\alpha, \tag{2}$$

and the sound power from the ideal component with amplitude I_T is given as

$$P_T=\int_0^{\pi}(I_T\cos^2\alpha)2\pi r_0^2\sin\alpha\, d\alpha=\frac{I_T}{3}(4\pi r_0^2). \tag{3}$$

The estimated intensity amplitude I_T for Fig. 2 is 1.70×10^{-7} W/m^2 for the observer radius of $r_0=0.5$ m, and the thrust sound power P_T is found to be 1.78×10^{-7} W, or SWL$=10\lg(P_T/10^{-12}\,\mathrm{W})=52.5$ dB. The difference between this sound power level and the actual rotary sound power level of 52.7 dB is 0.2 dB. The difference must be caused by an additional noise for which the sound power level is estimated as $10\lg(10^{5.27}-10^{5.25})=39.2$ dB. This additional noise is deemed to be uncontrollable. The difference between the overall noise and the synchronously averaged noise also represents the uncontrollable noise by the current method, but this part of the noise is mainly broadband and is not the focus of the present study.

The variation of sound radiation from one cycle to the next is studied by taking the Fourier transform for each cycle of the measured sound, which contains $B=7$ pressure oscillations for the BPF component. The temporal borders of each cycle are indicated by the tachometer signal taking into account the time required for sound propagation over a distance of $r_0=0.5$ m. The rms value of the BPF sound pressure varies with the cycle index n and is denoted as $p_{rms}(n)$, which is shown in Fig. 3 for the front, $\alpha=0°$, and the back of the fan, $\alpha=180°$. One possible reason for such variation is the change of local rpm with n. Assuming that the radiated sound power follows the usual sixth power law for dipoles, p_{rms} is proportional to $(\mathrm{rpm})^3$. The value of p_{rms} shown in Fig. 3 has already taken this into account by multiplying a factor of $(\mathrm{rpm}_0/\mathrm{rpm})^3$, where rpm_0 is the mean rpm and rpm is the actual rotational speed for cycle n. Thus corrected, the variation shown in Fig. 3 is believed to derive solely from the random aerodynamic events. The amplitude of noise from such random events is estimated as follows. If the random event contributes to the BPF noise with an rms amplitude A_r and the deterministic noise has an amplitude A_d, the range of the amplitude for the actual noise is, statistically, $[A_d-A_r, A_d+A_r]$. Here, A_d is found easily as the mean of the $p_{rms}(n)$ pattern shown in Fig. 3, i.e., $A_d=\overline{p_{rms}(n)}$, while A_r is found as $std(p_{rms})\sqrt{2}$. A_r is found to be roughly uniform over the whole measurement plane, so the sound power associated with the random events is calculated as $P_r=A_r^2 4\pi r_0^2/(\rho_0 c_0)$, which is found to be 38.4 dB, very close to the result of directivity pattern analysis shown in Eqs. (2) and (3). To summarize, the amount of uncontrollable rotary noise is about 39 dB and the maximum expected rotary sound power reduction is 52.7–39.0=13.7 dB. In terms of the percentage in sound power, the uncontrollable part represents $10^{-13.7/10}=0.043$ or 4.3%.

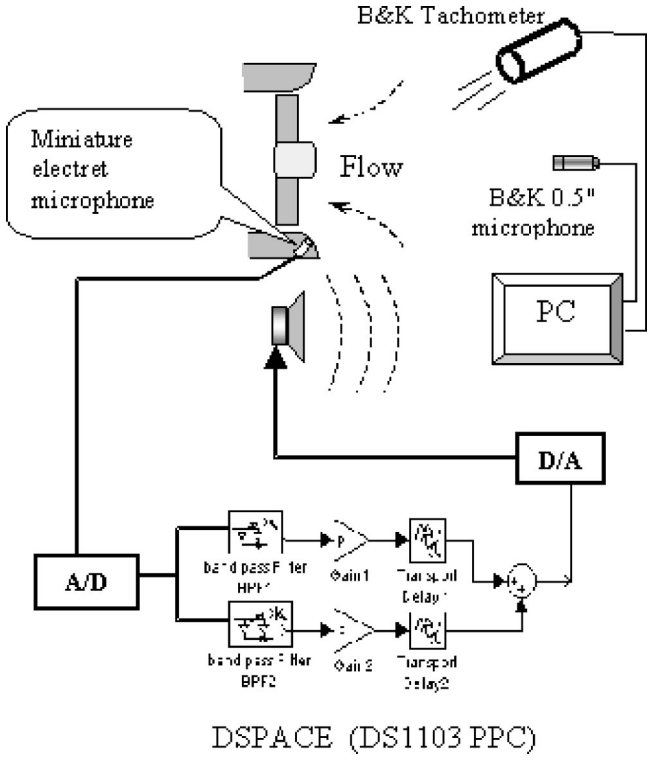

FIG. 4. Experimental setup in the anechoic chamber. The fan is isolated and unbaffled, and the secondary louderspeaker is put beneath the fan.

III. EXPERIMENTAL STUDIES

An open-loop, feed-forward control is used for the sample fan being investigated here. The system simply consists of three components. First, a nonacoustic reference from a miniature electret microphone, of which the details are described below, located on the bellmouth of the fan provides the clock information of the rotating fan blades. To some extent, the amplitude of the signal is also weakly related to the rotational speed. Second, the signal is bandpass filtered to keep the components of BPF and a few chosen harmonics, and further conditioned in terms of amplitude and phase delay. Third, the conditioned signal drives the loudspeaker attached just beneath the fan to produce the anti-sound to cancel out the noise made by the fan at the earliest possible blade passage cycle, which is $1/B$ of a rotational cycle. Note that for deterministic sound from the fan, the acoustic signal repeats B times during one rotational cycle. The total time delay of the system is found to be such that the signal from one moment is actually used to cancel noise at the next blade passage. Such a short time delay means that the limitation of the system performance is mainly rooted in the randomness of the aeroacoustic source. In what follows, the three elements of the control rig are discussed before the results are presented.

A. Experimental setup

The schematic diagram of the experiment is shown in Fig. 4. Illustrated at the upper-right corner are a $\frac{1}{2}$-in. survey microphone (B&K type 4187) and a tachometer (B&K type M004) connected to a PC equipped with signal analysis software MATLAB® and an A/D card. The survey microphone is not used as error sensor here but is merely for the purpose of evaluating the results. Note that this part of the experimental setup can be easily absorbed into the controller block shown in Fig. 4. It is kept as a separate part purely for operational convenience. The rig is built around a dSPACE (DS1103 PPC) controller, which is a real-time system with multiple A/D and D/A channels, and a Motorola PowerPC 604e microprocessor running at 333 MHz. The input signal derives from the rotation sensor and the output goes to the secondary sound source. The digital controller is connected to a personal computer through an ISA bus. The control algorithm is simply based on IIR filters constructed by the SIMULINK function in MATLAB® assembled in the host personal computer. A real-time interface (RTI) is used to build the code downloaded to and executed on the dSPACE hardware. The rotation sensor signal is sampled at 10 kHz, and the output analog signal is also constructed at an updating rate of 10 kHz, both deemed sufficient for the range of frequencies encountered in the current study. The control is concentrated on the most outstanding peaks on the fundamental BPF and its first harmonic, $m=1$, 2, at which the noise level exceeds the broadband by 17 and 14 dB, respectively. Two filters are constructed as parallel channels, one for each peak, to extract the rotational information at the two frequencies. Each channel has its own phase delay and amplification variables which can be adjusted manually in the computer to optimize the results. The outputs from the two channels are added together before the DA conversion.

The experiment is conducted in a full anechoic chamber with a cutoff frequency of 80 Hz, and the acoustic directivity is measured by the survey microphone fixed at one position 0.5 m away from the fan center, while the fan and loudspeaker rotate on a tripod to traverse all directions on the horizontal plane at an angular interval of 10°. The pulse signal from the optical tachometer is sampled together with that of the electret microphone by a 24-bit AD card using a sampling rate of 16 kHz. More details of the sensor microphone and other elements in the rig are discussed below.

B. Description of rig components

Normally, a photoelectric tachometer provides the information of the instantaneous position of the rotor by generating a pulse at each passing of a marked blade. Since the spectral energy of an ideal pulse (delta function) spreads out over a very wide frequency range, the amount of signal energy in one narrow band of frequency, such as that around the BPF, would be necessarily low in proportion. This makes it less ideal for the current purpose. In addition to this drawback, the height of the pulse is independent of the rotational speed, and it requires some kind of frequency to amplitude conversion if more antisound needs to be constructed to cancel the noise of the fan running at momentarily higher speed. In this study, a miniature electret microphone is used as the alternative rotation sensor. The microphone used is a 151 series from Tibbetts industries. It has a cylindrical head 0.1 in. in diameter and 3 mm in height, with a flat frequency response of 0.018 V/Pa from 300 Hz to 5 kHz. A photoelectric tachometer (B&K type MM0024) is also used in the rig and is located at some 30 cm upstream of the fan, while the

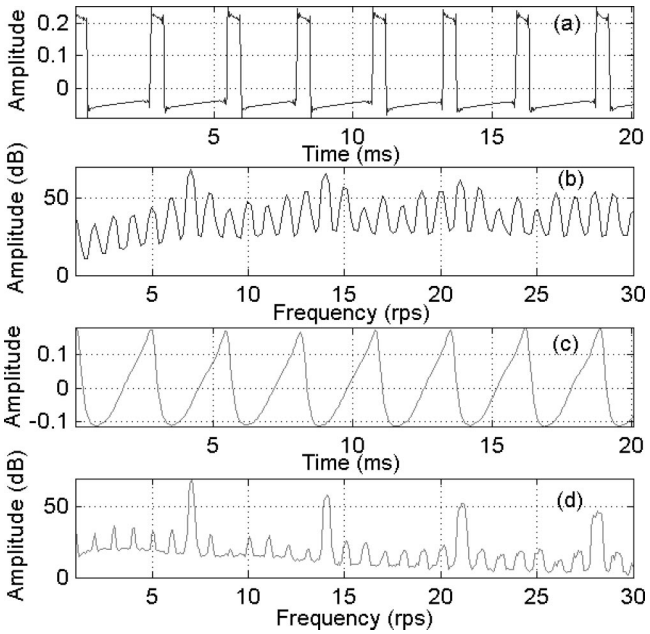

FIG. 5. Signals from two rotation sensors. (a) is for the photoelectric tachometer and (b) is the spectrum of signal in (a). (c) is the signal from the miniature microphone, and (d) its spectrum.

electret microphone is flush mounted on the inlet bellmouth of the fan just upstream of the blades. Signals from the photoelectric tachometer and the electret microphone are compared in Fig. 5. The photoelectric tachometer signal is shown in Fig. 5(a) and its spectrum in Fig. 5(b). Here, the ripples around the edges of the pulses are caused by the high-pass filter installed in the data acquisition system to avoid excessive electronic noise that exists at low frequencies. When the optical reflex paper is attached to all seven blades of the fan, the main peaks are found at the BPF and its harmonics. The appearance of the peaks at the rotational frequency (rps) and its non-BPF harmonics is caused by the difference among the pulses due to either the variation of tachometer or the changing fan rotational speed. The difference between the first BPF and its two neighboring non-BPF peaks is 16 dB.

Figure 5(c) shows the saw-tooth-like waveform from the electret microphone, and its spectrum is shown in Fig. 5(d). The BPF peak is cleared of its nearest non-BPF peaks by 35 dB. What is measured here is the aerodynamic pressure variation on the bellmouth surface caused by the constant sweeping of the blades, which is a source of far field sound but not all sound by itself. The effect of the blade rotation on the upstream flow is mainly a potential flow blockage, and its magnitude should be of the order of the dynamic pressure head associated with the velocity change during the sweeping. A brief test shows that the measured peak-to-peak pressure variation is 0.140, 0.154, and 0.162 Pa for the rotational speeds of 3000, 3100, and 3200 rpm, respectively. One suspected drawback of using the miniature microphone is that, in principle, the fan noise and antisound can also be sensed leading to a feedback loop in the system. But this worry is unfounded since the near-field amplitude of the loudspeaker sound is found to be around 5×10^{-3} Pa, which is much lower than the aerodynamic pressure amplitude, 162×10^{-3} Pa.

When the two signals in Figs. 5(a) and (c) are compared in terms of BPF energy contents, the tachometer has 23% while the electret microphone has 83%. The large spectral clearance between the BPF and its non-BPF neighbors for the electret microphone means that the passband of the filter does not have to be too narrow in order to extract the BPF signal. In fact, a very wide band of 200–500 Hz is used in the current study for the BPF around 373 Hz. This way, the time delay caused by the filtering is minimal, and the effect of noise cancellation is expected to be much better than that based on the photoelectric tachometer. In addition to this crucial time-delay factor, the use of a miniature microphone is also more economical and convenient. A much broader bandpass filter also allows simpler analog construction in future applications. In terms of the secondary source, a 4-in. loudspeaker is used, and its dipole directivity is confirmed by the measurement without the fan. Also, the loudspeaker is found to have a time delay of 0.4 ms at the frequency of the BPF for which the period is 2.7 ms.

The overriding consideration for the filter design is the time delay caused by the filter. A time delay here means that the signal of the rotational sensor at present is used to construct antisound for the future. The random variation of the BPF amplitude with respect to the rotational cycle shown in Fig. 3 means that such delay should be minimized in order to achieve the best result. Since an infinite-impulse-response (IIR) filter has much smaller time delay than a finite-impulse-response (FIR) filter with equivalent bandpass performance, the former is chosen. In making this choice, the factor of signal distortion by the IIR filter is not much a factor for the following reason. There is no reason to assume that the time delay between the component of BPF in the rotational signal shown in Fig. 5(c) and the radiated sound is the same as that for the second BPF component. In other words, the required time delays for the fundamental ($m=1$) and first harmonic ($m=2$) may well be different. In fact, due to the variation of the rotational speed of the fan, the ideal antisound should maintain a fixed phase angle of 180° with respect to the original noise at its varying BPF and higher harmonics. The varying phase relation between the sensor signal and the final antisound for various frequencies means a nonlinear phase response might well be ideal. In this study, such nonlinear phase response is not studied, nor is the varying amplitude response that might be beneficial.

As shown in Fig. 5, the sharp BPF peak allows a wide passband to be used together with a wide transitional band. This allows a low-order filter to be constructed to achieve a flat response. For the fan operating at 3200 rpm, 373 Hz is the fundamental BPF, and 200–550 Hz is chosen as the passband with its center at 375 Hz. The band of 600 to 900 Hz is chosen for the first harmonic with its center at 750 Hz. A six-order Chebyshev IIR filter is constructed by using the least *p*-norm optimal IIR filter design in the SIMULINK of MATLAB®, and the responses of the two filters are shown in Fig. 6. Based on these filters, a further gain and phase delay are required to construct the antisound, as shown in the lower part of Fig. 4. These are achieved by manual tuning for the two channels independently, although there is no reason why a formal procedure of system identification cannot be

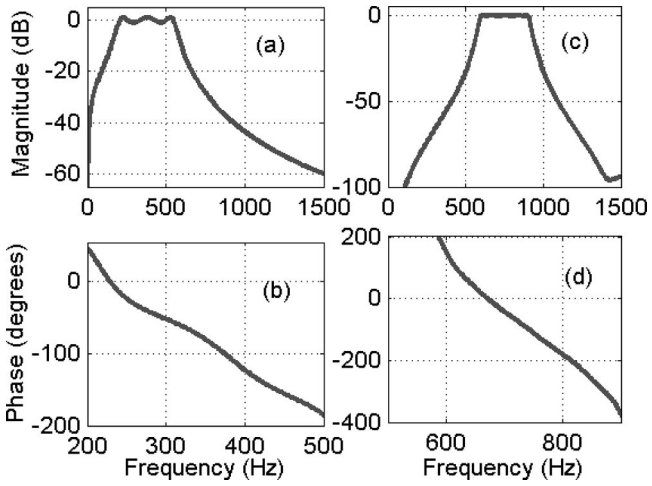

FIG. 6. The responses of the two filter channels. (a) and (b) are the magnitude and phase response for the first BPF, respectively, (c) and (d) are for the second.

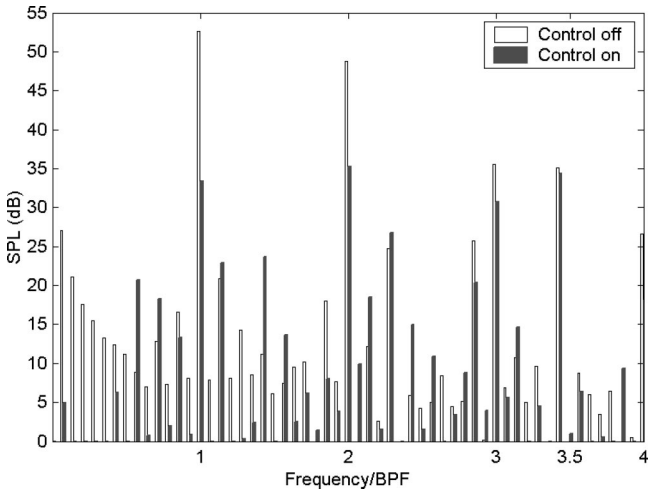

FIG. 7. Sound pressure spectra at the on-axis peaks of dipole with control off (open bar) and on (filled bar).

followed to achieve the goal of noise minimization. The manual tuning is based on the display of sound picked up by the survey microphone on the rotational axis, $\alpha=0$.

C. Results and error analysis

The loudspeaker is put underneath the fan to minimize its influence on the incoming flow stream. The dipole sound from the fan and that from the loudspeaker are coupled as an effective lateral quadrupole with a perpendicular separation distance of $d=10$ cm between the two parallel dipole axes. The ratio of the quadrupole sound power to the dipole sound power can be shown to be $(kd)^2/5$ (Dowling, 1998), where $k=2\pi f/c_0$ is the wave number. For frequency $f=373$ Hz, the ratio turns out to be 0.096, which means a maximum reduction of sound power of $-10\lg(0.096)=10.2$ dB. This is a serious limiting factor. Ideally, a ring of small loudspeakers should be placed around the fan circumference in order to create a better coincidence of the centers of the two noise sources. In practice, two or four loudspeakers might be adequate. Using simple numerical simulation of linear superposition of sounds from two antisound speakers placed at the top and the bottom of the fan, which is itself modeled by seven-point dipoles on a ring of 4.5-cm radius, it is found that the best cancellation is improved to become 24.1 dB, which is quite satisfactory. So, the issue of the relatively large fan-loudspeaker separation distance is temporarily set aside by the following heuristic method. The parameters of the antisound are tuned only on the horizontal plane level with the fan center, and the finalized result is also measured on the same plane. In terms of the separation of the primary and secondary sources, the method of shaking the fan itself as a secondary source (Lauchle *et al.*, 1997) may have achieved a rather perfect collocation. The only limitation factor for the performance becomes the issue of whether the primary and secondary sources have the same dipole composition and acoustic directivity pattern.

The spectra of synchronous sound measured with and without the loudspeaker for $\alpha=0$ are presented in Fig. 7. It is found that 18.5-dB noise reduction is achieved for the first BPF, and 13.0 dB for the second BPF. There is also a peak at approximately 3.5 BPF, for which there is virtually no change in sound pressure level. This source of this peak is beyond the scope of the current investigation. Acoustic directivity is also measured on the horizontal plane level with the center of the fan, and the control on–off comparison of sound intensity is made in Fig. 8. Figure 8(a) compares the total synchronous sound pressure levels in decibel units, with the total sound powers labeled on the horizontal axis. Figure 8(b) gives the details of the control-on directivity, which includes the overall noise, rotary noise, and the random noise derived from, respectively, the original signal measured from the survey microphone, the synchronous average of the measured signal, and the power difference between the original

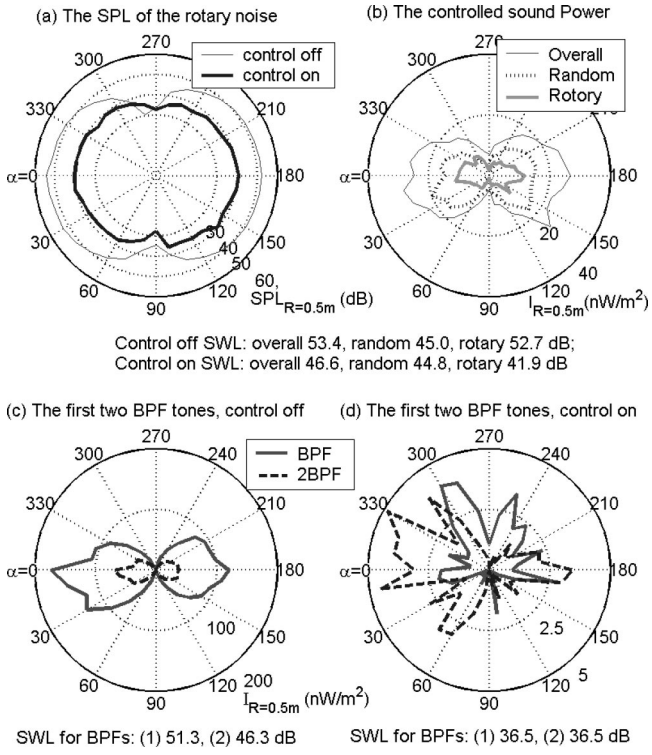

FIG. 8. Sound power level comparisons for with and without control.

and synchronous signals. Note that the rotary noise includes sound at frequencies other than the harmonics of BPF, such as 3.5 BPF shown in Fig. 7. The total reduction in the rotary noise power is $52.7-41.9=10.8$ dB. The overall noise reduction is $53.4-46.3=7.1$ dB while the random noise, about 50.0 dB, is essentially unchanged.

Figures 8(c) and (d) show the sound intensity directivity of the BPF and 2 BPF noise for control-off and control-on, respectively. While the control-off pattern is clearly an axial dipole with some limited distortions, the control-on pattern is quite irregular and the scale for this figure is amplified by 40 times when compared with Fig. 8(c). The irregular shape indicates that most harmonic noise that can be controlled by the simple scheme has already been suppressed successfully. The sound power reductions for the two frequencies are 14.8 and 9.8 dB, respectively.

The result of this simple control scheme is determined by many factors, and the main one has been recognized earlier as the random variation of sound radiation by the rotating fan (see Fig. 3). The standard deviation of sound pressure amplitude is 15.9% while that for the rpm is 0.4%. If the radiated sound pressure grows with rpm by the third power law, the variation in the sound pressure amplitude would have been only $3\times0.4=1.2\%$. The difference between this prediction and the actual 5.6% change in the radiated sound amplitude means that the variation is rather independent of the rotational speed change. In fact, the correlation study between one-cycle p_{rms} and rpm^3 shows a peak correlation of only 20%. The deterministic error of using the rotational signal from one blade passage to control the noise radiated by the next blade passage is also analyzed in terms of the phase error due to the response characteristics of the filter shown in Fig. 6(b). The error of 0.4% BPF period means a frequency error of $0.004\times373=1.5$ Hz, or a phase response difference of $\delta\theta=1.5°$ based on the phase response curve in Fig. 6(b). This phase angle error can only lead to an error of $\delta\theta$ in radian units, which is 0.026 or a limit of noise reduction of $-20\lg(0.026)=31.7$ dB, which is also unlikely to be a bottleneck of the performance.

IV. CONCLUSIONS

The reported scheme of active acoustic interference demonstrates that the sound locked with the rotation from the typical computer cooling fan can be significantly attenuated by a simple design. More specifically, the following conclusions are drawn.

(1) The noise of the sample computer cooling fan is sufficiently deterministic to allow a meaningful implementation of the proposed scheme. For the dominant BPF sound, it is shown that the noise associated with the seemingly random variation of sound radiation with respect to the fan rotation is about 13.7 dB below that of the deterministic part. In other words, 95.7% of sound energy is deterministic, and the maximum expected noise reduction is 13.7 dB. The experimental rig deals with the first and second BPF frequencies. The reductions in the total sound power for these frequencies are 10.4 and 9.8 dB, respectively, while the total synchronous sound is reduced by 10.8 dB. The reduction of the sound power in the experiment for the BPF, 10.8 dB, is close enough to the limit of 13.7 dB forecasted for the deterministic acoustic interference.

(2) The cause of the random variation could have a complex origin in turbulent fluid dynamics, and the limitation imposed by this factor is much more stringent than those imposed by the known phase delay and amplitude mismatch problems associated with the inevitable variation of the fan rotational speed from one cycle to the next. In fact, this variation is rather small since the total time delay involved in the current study is only about half of the blade passage, or $\frac{1}{14}$ of the rotational cycle. A more stringent limitation appears to be the separation distance between the fan center and the single loudspeaker, but this problem would be alleviated if two loudspeakers are used.

(3) If the rotation signal is provided by a traditional photoelectric tachometer, the pulse signal does not carry sufficient BPF content and it would limit the performance of the method. In this study, a miniature electret microphone is used to provide the unsteady pressure arising from the blade rotation just upstream of the rotor. The signal is found to be very rich in BPF content and is rather smooth. Spectral analysis shows that the peak at the BPF is well above the neighboring rps harmonics. As a result, a broad passband can be used to extract the BPF signals to drive the loudspeaker. The time delay for the filter is thus minimized. Apart from this technical advantage, the miniature microphone is also relatively cheap and small to allow the implementation of the technique in practice.

(4) The sample fan used in this study is a modified version of a typical computer cooling fan. In a typical fan, the number of struts differs from the number of rotor blades, $S\neq B$. It is pointed out in this study that this seemingly correct design avoids the worst coincident mode sound radiation by the unsteady flow thrust, but it is almost impossible to avoid the equally efficient radiation of drag noise. Since drag noise originates from a rotating dipole with a changing dipole axis, the modification from the usual design with drag noise domination to the coincident design of $S=B$ with thrust noise domination carries the following important technical advantage: a simple loudspeaker can be used as the secondary source for the thrust noise but the same cannot be done easily for the drag noise.

ACKNOWLEDGMENTS

The first author thanks the Hong Kong Polytechnic University for the Ph.D. research studentship. The support by the Research Grants Council of the Government of HKSAR (Grant No. PolyU 1/02C) is also gratefully acknowledged.

Blake, W. K. (**1986**). *Mechanics of Flow-induced Sound and Vibration* (Academic, Orlando, FL).

Dowling, A. P. (**1998**). "Steady-state radiation from sources," in *Handbook of Acoustics*, edited by M. J. Crocker (Wiley, New York), Chap. 8.

Envia, E., and Nallasamy, M. (**1999**). "Design selection and analysis of a swept and leaned stator concept," J. Sound Vib. **228**, 793–836.

Ffowcs Williams, J. E., and Hall, L. H. (**1970**). ''Aerodynamic sound generation by turbulent flow in the vicinity of a scattering half plane,'' J. Fluid Mech. **40**, 657–670.
Ffowcs Williams, J. E., and Hawkings, D. L. (**1969**). ''Sound generation by turbulence and by surfaces in arbitrary motion,'' Philos. Trans. R. Soc. London, Ser. A **264**, 321–342.
Fitzgerald, J. M., and Lauchle, G. C. (**1984**). ''Reduction of discrete frequency noise in small, subsonic axial-flow fans,'' J. Acoust. Soc. Am. **76**, 158–166.
Fukano, T., Takamatsu, Y., and Kodama, Y. (**1986**). ''The effects of tip clearance on the noise of low pressure axial and mixed flow fans,'' J. Sound Vib. **105(2)**, 291–308.
Gerhold, C. H. (**1997**). ''Active control of fan-generated tone noise,'' AIAA J. **35**, 17–22.
Gutin, L. (**1936**). ''On the sound field of a rotating propeller,'' Zh. Tekh. Fiz. **6**, 899–909.
Howe, M. S. (**1998**). *Acoustics of Fluid-structure Interaction* (Cambridge U.P., Cambridge).
Huang, L. (**2003**). ''Characterizing computer cooling fan noise,'' J. Acoust. Soc. Am. **114**, 3189–3199.
Kemp, N. H., and Sears, W. R. (**1953**). ''Aerodynamic interference between moving blade rows,'' J. Aeronaut. Sci. **20**, 583–598.
Kemp, N. H., and Sears, W. R. (**1955**). ''Unsteady forces due to viscous wakes in turbomachines,'' J. Aeronaut. Sci. **22**, 478–483.
Lauchle, G. C., Macgillivray, J. R., and Swanson, D. C. (**1997**). ''Active control of axial-flow fan noise,'' J. Acoust. Soc. Am. **101**, 341–349.
Lighthill, M. J. (**1952**). ''On sound generated aerodynamically. I. Genera theory,'' Proc. Annu. Tech. Meet., Tech. Assoc. Graphic Arts **211**, 564–587.
Longhouse, R. E. (**1976**). ''Noise mechanism separation and design considerations for low tip-speed, axial-flow fans,'' J. Sound Vib. **48**, 461–474.
Longhouse, R. E. (**1978**). ''Vortex shedding noise of low tip speed, axial flow fan,'' J. Sound Vib. **53**, 25–46.
Lowson, M. V. (**1965**). ''The sound field for singularities in motion,'' Proc. R. Soc. London, Ser. A **286**, 559–572.
Lowson, M. V. (**1970**). ''Theoretical analysis of compressor noise,'' J. Acoust. Soc. Am. **47**, 371–385.
Majumdar, S. J., and Peake, N. (**1998**). ''Noise generation by the interaction between ingested turbulence and a rotating fan,'' J. Fluid Mech. **359**, 181–216.
Morfey, C. L. (**1973**). ''Rotating blades and aerodynamic sound,'' J. Sound Vib. **28**, 587–617.
Nauhaus, L., Schulz, J., Neise, W., and Moser, M. (**2003**). ''Active control of the aerodynamic performance and tonal noise of axial trubomachines,'' Proc. Inst. Mech. Eng., Part A: J. Power and Energy **217**, 375–383.
Quinlan, D. A. (**1992**). ''Application of active control to axial flow fans,'' Noise Control Eng. J. **39**, 95–101.
Rao, N. M., Feng, J. E., Burdisso, R. A., and Ng, W. F. (**2001**). ''Experimental demonstration of active flow control to reduce unsteady stator-rotor interaction,'' AIAA J. **39**, 458–464.
Sharland, I. J. (**1964**). ''Sources of noise in axial flow fan,'' J. Sound Vib. **I(3)**, 302–322.
Simonich, J., Lavrich, P., Sofrin, T., and Topol, D. (**1993**). ''Active aerodynamic control of wake-airfoil interaction noise—experiment,'' AIAA J. **31**, 1761–1768.
Thomas, R. H., Burdisso, R. A., Fuller, C. R., and O'Brien, W. F. (**1993**). ''Preliminary experiments on active control of fan noise from a turbofan engine,'' J. Sound Vib. **161(3)**, 532–537.
Thomas, R. H., Burdisso, R. A., Fuller, C. R., and O'Brien, W. F. (**1994**). ''Active control of fan noise from a turbofan engine,'' AIAA J. **32**, 23–30.
Trunzo, R., Lakshminarayana, B., and Thompson, D. E. (**1981**). ''Nature of inlet turbulence and strut flow disturbances and their effect on turbomachinery rotor noise,'' J. Sound Vib. **76(2)**, 233–259.
Tyler, J. M., and Sofrin, T. G. (**1962**). ''Axial flow compressor noise studies,'' SAE Trans. **70**, 309–332.
Wong, J., and Huang, L. (**2003**). ''Identification and control of noise sources in a small axial-flow cooling fan,'' Symposium on Fan Noise 2003, Senlis, France, 23–25 September.